Supporting Information

An All-Fluorinated Ester Electrolyte for Stable High-Voltage Li Metal Batteries at Ultra-Low Temperature

John Holoubek[a,‡], Mingyu Yu[b,‡], Sicen Yu[b], Minqian Li[c], Zhaohui Wu[c], Dawei Xia[a], Pranjal Bhaladhare[a], Matthew S. Gonzalez[a], Tod A. Pascal[a,c], Ping Liu[a,b,c,d], Zheng Chen[a,b,c,d]*

[a]*Department of NanoEngineering, University of California, San Diego, La Jolla, CA 92093, USA*

[b]*Program of Materials Science, University of California, San Diego, La Jolla, CA 92093, USA*

[c]*Program of Chemical Engineering, University of California, San Diego, La Jolla, CA 92093, USA*

[d]*Sustainable Power and Energy Center, University of California, San Diego, La Jolla, CA 92093, USA*

[‡]*These authors contributed equally*

**Email: zhengchen@eng.ucsd.edu*

Materials Synthesis and Fabrication

For battery electrode preparation, $LiNi_{0.8}Co_{0.1}Mn_{0.1}O_2$ (NMC 811), powder was purchased from Targray Technology International Inc. The cathode slurries were prepared by mixing NMC 811, super-P, and polyvinylidene fluoride (PVDF, KYNAR 2800) (8:1:1 mass ratio) in N-methyl pyrrolidone (NMP, Sigma Aldrich > 99.5%), which was then cast on Al foil and dried overnight under vacuum at 80 ^oC. Blocking electrodes for electrolyte stability determination were prepared by mixing super-P and PVDF (9:1 mass ratio) in NMP, which was then cast on stainless steel and dried under vacuum at 80 ^oC overnight.

For electrolyte preparation, fluoroethylene carbonate (FEC, > 98%) was purchased from Alfa Aesar, methyl 3,3,3-trifuoloropropionate (MTFP, > 98%) was purchased from TCI, $LiPF_6$ (99.99%) was purchased from BASF, methyl propionate (MP, > 99%) and 1 M $LiPF_6$ in ethylene

carbonate/diethyl carbonate (EC/DEC 1:1, battery grade) were purchased from Sigma Aldrich. MP and MTFP solvents were dried over molecular sieves for at least 24 hr before use in electrolytes. Low-temperature electrolytes were made by dissolving stoichiometric amounts of $LiPF_6$ in the selected solvents under stirring.

Materials Characterization

The ionic conductivity of the electrolyte was measured by a customized two-electrode coin cell, in which the two stainless-steel electrodes are spaced symmetrically between a polytetrafluoroethylene washer with a thickness of 0.030 inches. A glass-fiber separator soaked with electrolyte was housed on the inside of the washer, constraining its surface area to a known value. The electrolytic conductivity value was then obtained with electrochemical impedance spectroscopy (EIS) using the following equation: $\sigma = \frac{L}{A * R}$, where R is the measured ionic resistance and A and L are the area of and space between the electrodes, respectively. The low temperature data points were collected inside of a SolidCold C4-76A ultra-low chest freezer.

X-ray photoelectron spectroscopy (XPS) (Kratos Analytical, Kratos AXIS Supra) was carried out using an Al anode source at 15 kV and all the peaks were fitted based on the reference C-C bond at 284.6 eV in CasaXPS. All XPS measurements were collected using a charge neutralizer during acquisition. Survey scans were collected with a 1.0 eV step size, and were followed by high resolution scans with a step size of 0.1 eV for C 1s, O 1s, F 1s, and P 2p regions. X-ray diffraction (XRD) measurements were carried out on a Bruker D2 Phaser (Cu Kα radiation, λ = 1.5406 Å) from $2\Theta = 10 - 80^{o}$ at a scan rate of 1.2^{o} min^{-1}.

Electrochemical Measurement

To evaluate the electrochemical performance, the prepared electrodes were fabricated into two-electrode CR-2032 type coin cells. Half-cells were evaluated with the electrolyte of interest using a Celgard 2400 poly-propylene membrane as the separator and Li metal (China Energy Lithium Co., 99.9%) as the counter electrode, where the working electrode had a typical mass loading of 0.84 mAh cm^{-2}. Full-cells were evaluated in a similar fashion, where the limited Li metal anode was prepared via electrodeposition in Li||Cu coin cells prior to application in full-cells, where the plated Li anode was paired with a NMC811 cathode of 1.3 mAh cm^{-2} loading. The theoretical capacity of NMC 811 was set to 200 mAh g^{-1} for the C-rate determination. All charge/discharge testing was performed on Neware BTS 4000 or Arbin LBT-10V5A systems.

The electrochemical stability of the electrolytes was investigated in coin cells using linear scan voltammetry (LSV) of a super-P/PVDF working electrode vs. a Li metal counter on a Biologic VSP-300 potentiostat at 1 mV s^{-1}. For low temperature electrochemical tests, the half-cells were first cycled for 2 times at room temperature with a rate of 0.2 C. The cells were then charged at 0.1 C at room temperature, placed into the temperature chamber and allowed to rest for 2 hours to reach the set temperature, followed by discharging at various rates. The SolidCold C4-76A ultra-low chest freezer with a secondary insulation chamber was used to maintain the cells at a specified temperature. EIS was performed on half-cells using a Biologic VSP-300 potentiostat from 1 MHz to 100 mHz with an AC amplitude of 10 mV. Symmetric cathode cells for EIS tests were first assembled in Li||NMC 811 half cells and cycled twice at 0.2 C before being brought to 50% state-of-charge and disassembled, followed by reassembly in symmetric cells.

Computational Methods

Density Functional Theory (DFT) calculations were performed in Gaussian 09. Single molecules were assembled and subjected to gas-phase DFT geometry optimization using the augmented polarized triple-ξ 6-311G+ (3df,2p) basis set from Pople and coworkers[1] and the B3LYP[2] functional, a well-balanced level of theory providing a reasonable compromise between speed and accuracy. Molecular Dynamics (MD) simulations were performed in LAMMPS using the 2019 General Amber Force-field (GAFF19), with atom parameters generated by the ANTECHAMBER program for the solvent molecules, and the PF_6^- parameters proposed by Kumar *et al*.[3] on simulation boxed containing 20 $LiPF_6$ molecules, and 85 EC/87 DEC, 223 MP/13 FEC, and 98 MTFP/13 FEC molecules representing 1 M $LiPF_6$ EC/DEC (1:1), 1 M $LiPF_6$ MP/FEC (9:1), and 1 M $LiPF_6$ MTFP/FEC (9:1), respectively. In all cases the charges of the Li^+ and PF_6^- molecules were scaled to the high-frequency dielectric properties of the solvents present in the system according to the method proposed by Park *et al*.[4] For each system, an initial energy minimization at 0 K (energy and force tolerances of 10^{-4}) was performed to obtain the ground-state structure. After this, the system was slowly heated from 0 K to room temperature at constant volume over 0.02 ns using a Langevin thermostat, with a damping parameter of 100 ps. The system was then subjected to 5 cycles of quench-annealing dynamics, where the temperature was slowly cycled between 298 K and 894 K over 0.08 ns in order to eliminate the persistence of any meta-stable states. After annealing, the system was equilibrated in the constant temperature (298 K), constant pressure (1bar) (NpT ensemble) for 0.05 ns before finally being subjected to 0.5 ns of constant volume, constant temperature dynamics. Radial distribution functions were obtained using the Visual Molecular Dynamics (VMD) software.

Table S1. Physical properties of organic solvents obtained from Ref. [5] unless specified otherwise.

Solvent	Melting Pt.	Boiling Pt.	Room Temp Viscosity	Dielectric Const. (ε)
Ethylene Carbonate (EC)	36.4 °C	212 °C	1.95 (@ 40°C)	89.8
Fluoroethylene Carbonate (FEC)[6]	20 °C	243 °C	3.98	109.4
Propylene Carbonate (PC)	-48.8 °C	240 °C	2.20 cP	66.2
Diethyl Carbonate (DEC)	-43.0°C	126 °C	0.77 cP	2.82
Methyl Propionate (MP)	-87.5 °C	79.8 °C	0.43 cP	6.20

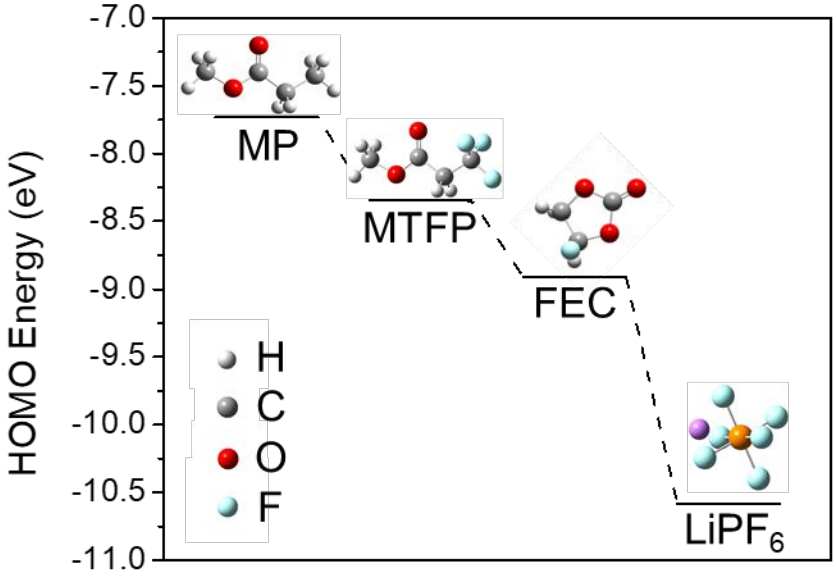

Figure S1. HOMO levels obtained from DFT calculations of individual electrolyte components.

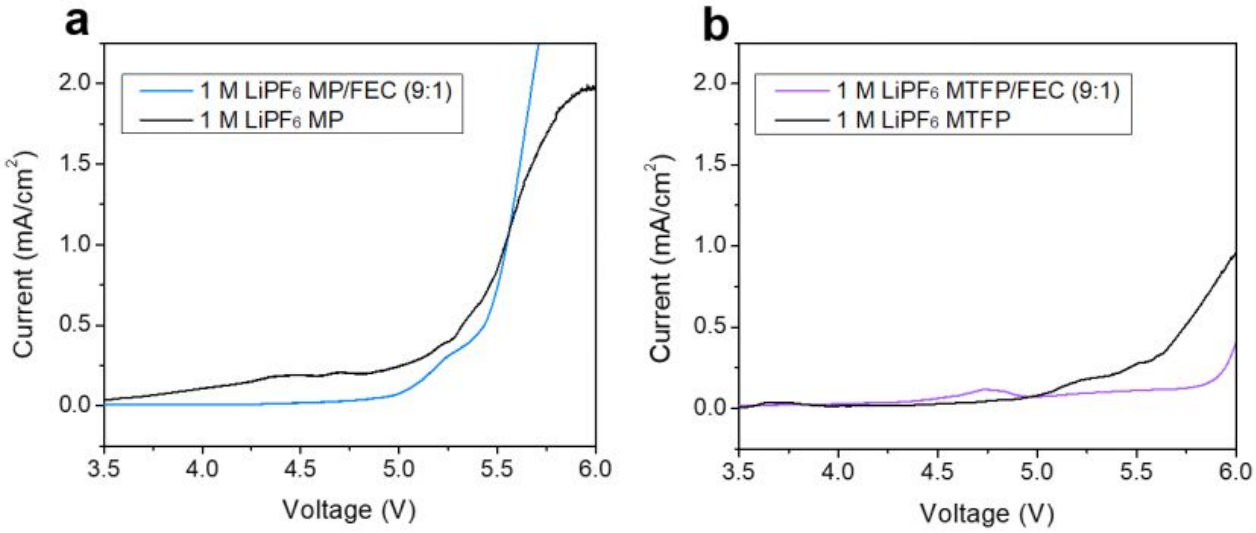

Figure S2. LSV profile comparison of conductive carbon electrodes in selected ester electrolytes with and without FEC at 1 mVs^{-1}. **a)** MP/FEC. **b)** MTFP/FEC.

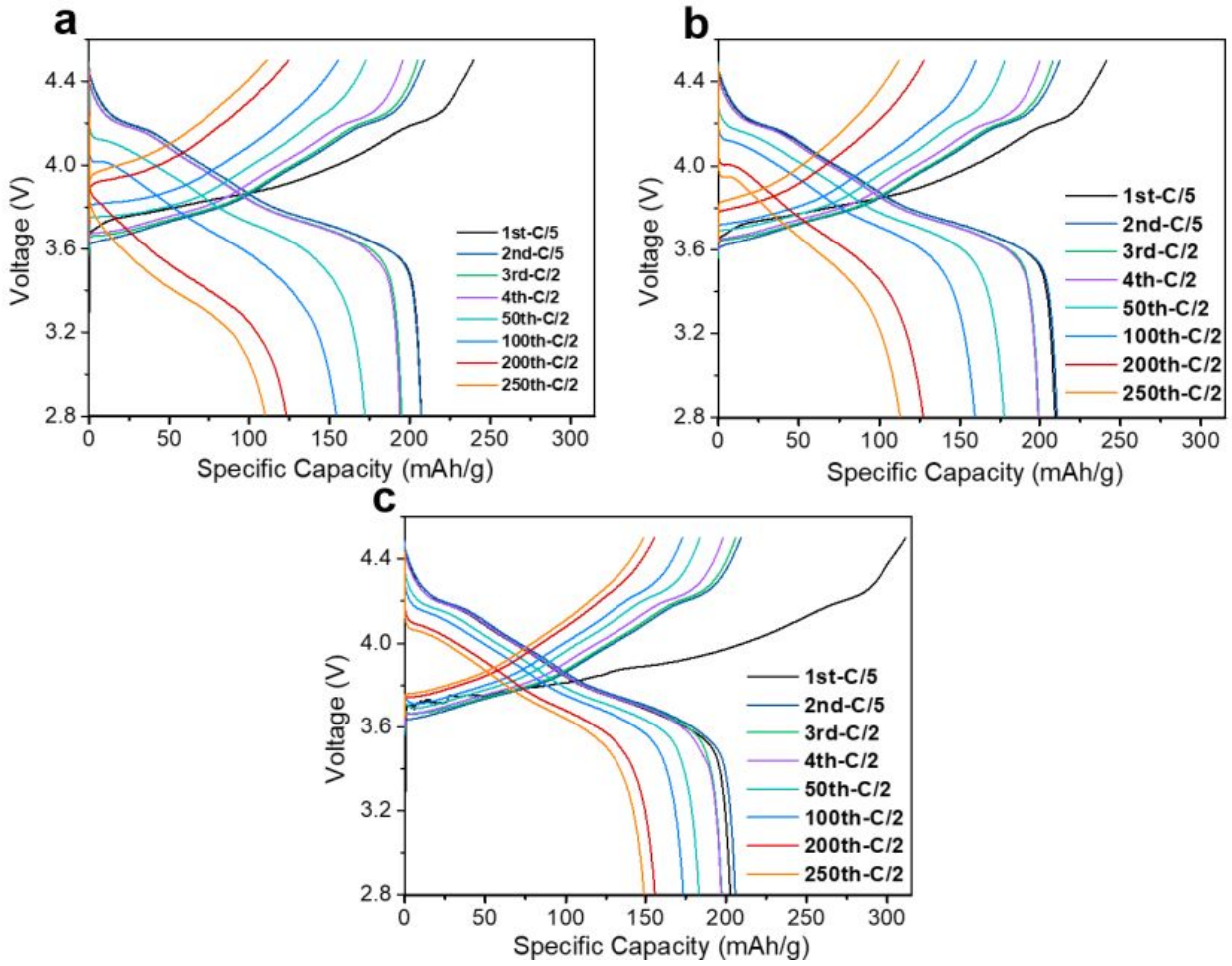

Figure S3. Voltage profiles of NMC811||Li half cells during cycling in selected electrolytes at room temperature. **a)** 1M $LiPF_6$ EC/DEC. **b)** 1M $LiPF_6$ MP/FEC. **c)** 1M $LiPF_6$ MTFP/FEC.

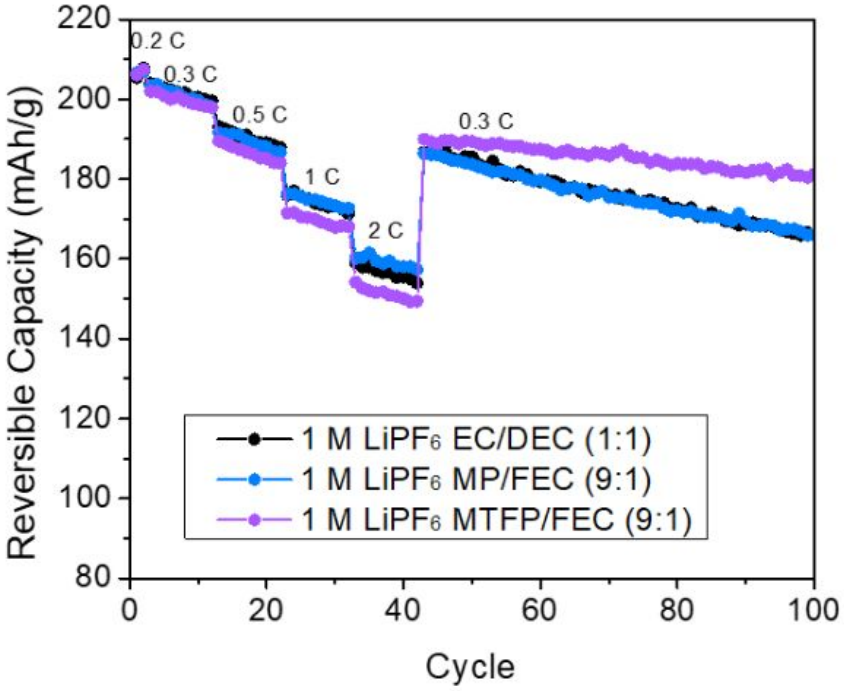

Figure S4. Rate performance of NMC811||Li half cells with selected electrolytes at room temperature.

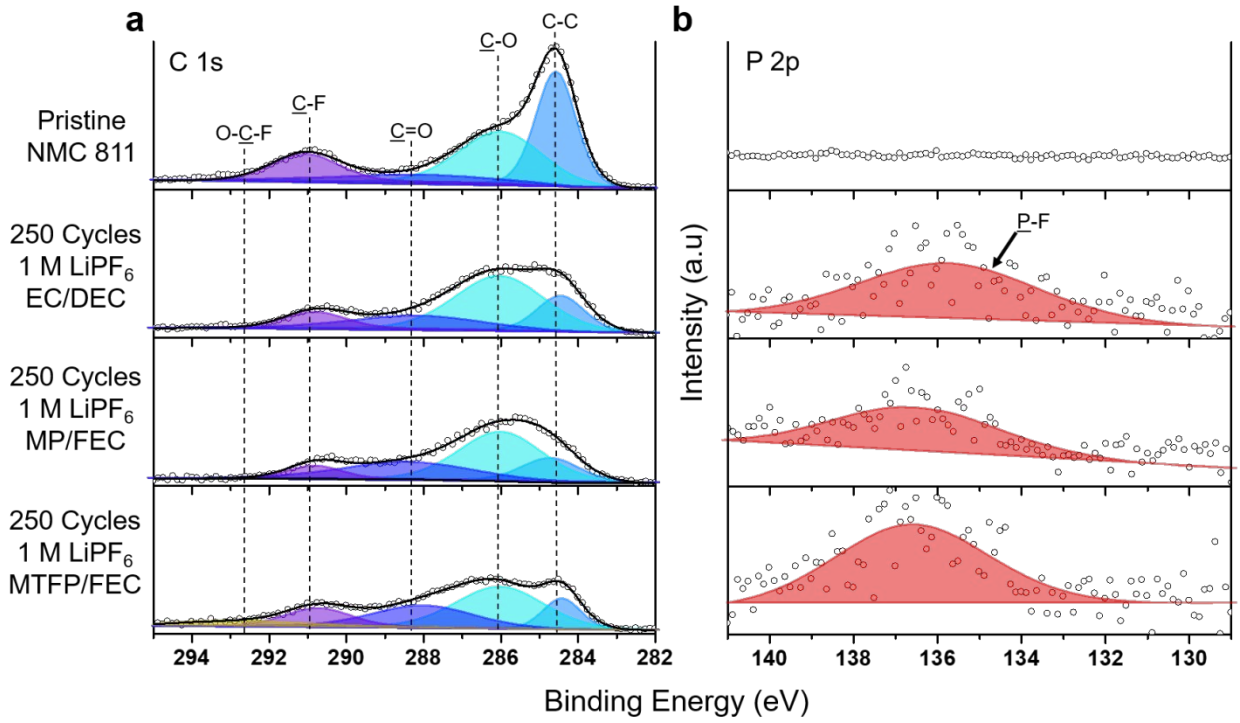

Figure S5. XPS spectra of the **a)** C 1s and **b)** P 2p regions taken from the NMC811 cathodes in selected electrolytes.

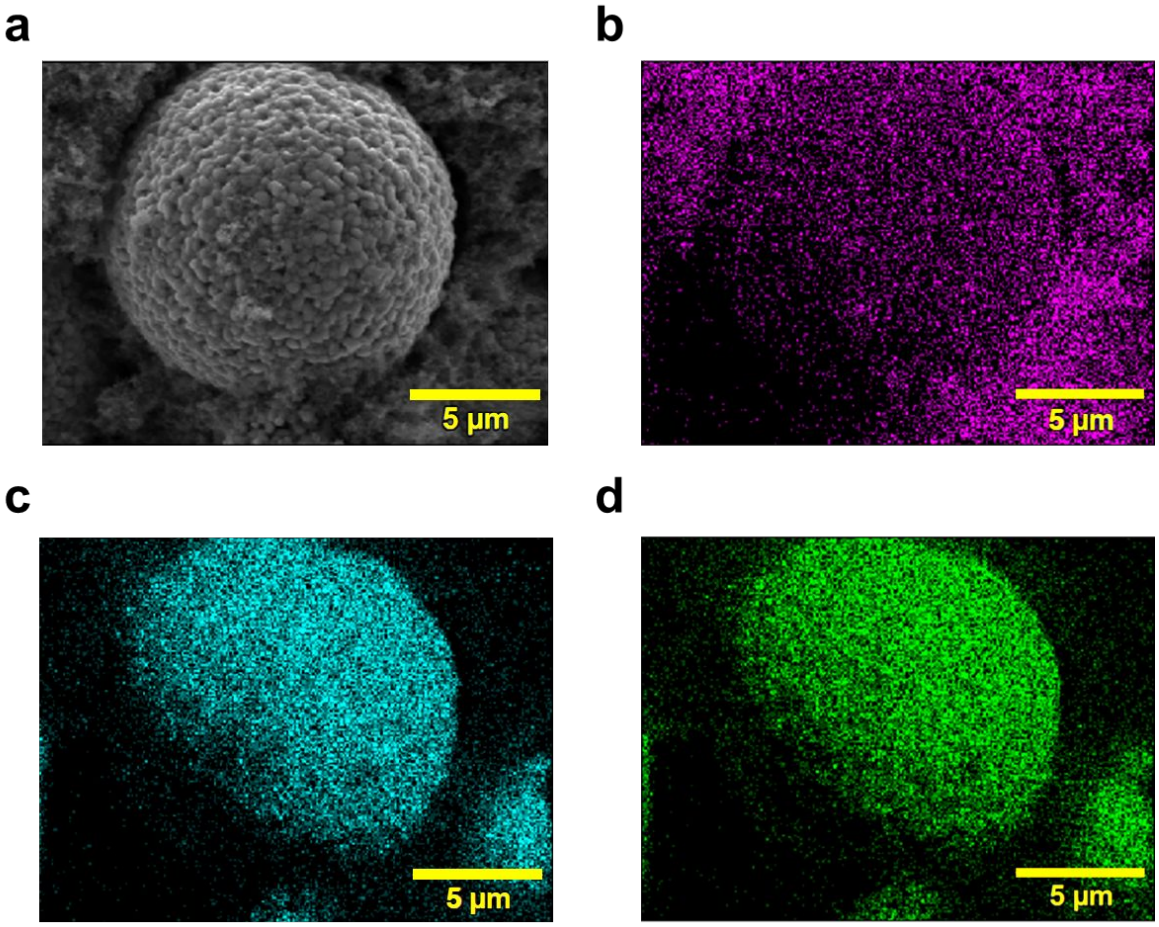

Figure S6. *Ex-Situ* SEM and Energy Dispersive X-Ray Spectroscopy (EDX) of a representative NMC 811 particle after 250 cycles in 1 M $LiPF_6$ MTFP/FEC (9:1). **a)** SEM image, and EDX mapping of **b)** Fluorine, **c)** Oxygen, and **d)** Nickel.

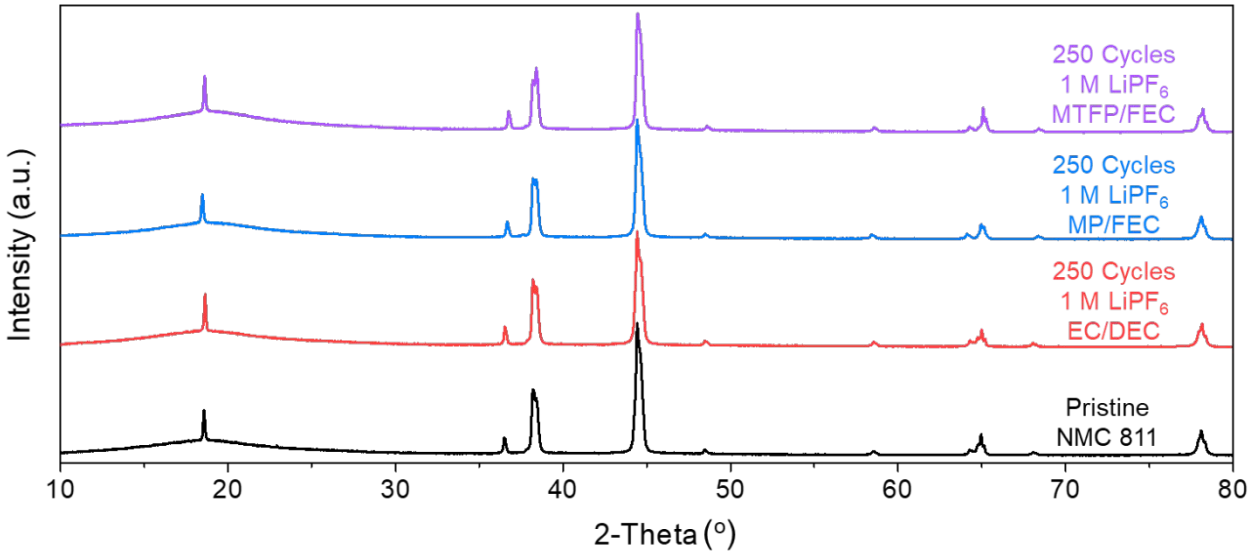

Figure S7. *Ex-Situ* XRD patterns of the pristine NMC811 cathode and the cycled NMC811 cathodes (250 cycles at 0.5C and room temperature) in selected electrolytes.

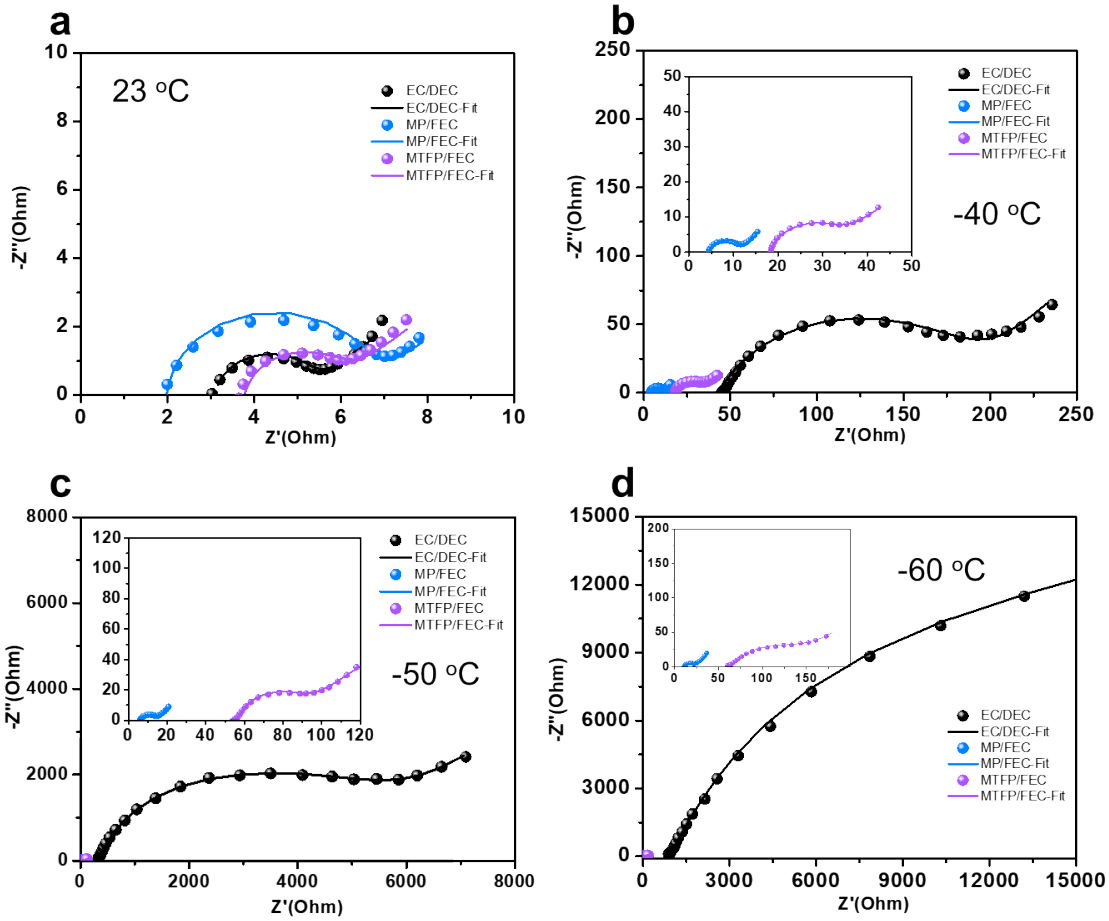

Figure S8. Nyquist Impedance plots of symmetric NMC 811 || NMC 811 cells at 50% SOC taken at a temperature of **a)** 23 °C, **b)** -40 °C, **c)** -50 °C, **d)** -60 °C.

References

[1] W. J. R. Hehre, P. v. R. Schleyer, and J. A. Pople, *Ab Initio Molecular Orbital Theory* Wiley, New York, 1986.

[2] G. J. Laming, V. Termath, N. C. Handy, *J. Chem. Phys.* **1993**, *99*, 8765–8773.

[3] N. Kumar, J. M. Seminario, *J. Phys. Chem. C* **2016**, *120*, 16322–16332.

[4] C. Park, M. Kanduč, R. Chudoba, A. Ronneburg, S. Risse, M. Ballauff, J. Dzubiella, *Journal of Power Sources* **2018**, *373*, 70–78.

[5] D. R. L.-T. J. B.-T. & F. Group, *CRC Handbook of Chemistry and Physics, 95th Edition, CRC Press, 2014: CRC Handbook of Chemistry and Physics*, **2014**.

[6] M. Ohtake, N. Nanbu, M. Takehara, M. Ue, Y. Sasaki, *ECS Meet. Abstr.* **2008**, *MA2008-02*, 175–175.